Ultrafast Quantitative Ultrasound and Shear Wave Elastography Imaging of *In Vivo* Duck Fatty Liver

Marc Gesnik[1], Manish Bhatt[1], Marie-Hélène Roy-Cardinal[1], François Destrempes[1], Boris Chayer[1], Louise Allard[1], An Tang[2,3,4], and Guy Cloutier[1,3,4]

1 Laboratory of Biorheology and Medical Ultrasonics, University of Montreal Hospital Research Center, Montreal, Quebec, Canada
2 Clinical Laboratory of Image Processing, University of Montreal Hospital Research Center, Montreal, Quebec, Canada
3 Institute of Biomedical Engineering, University of Montreal, Montreal, Quebec, Canada
4 Department of Radiology, Radio-Oncology and Nuclear Medicine, University of Montreal, Montreal, Quebec, Canada

Abstract— **Multi-parametric ultrasound imaging is a promising tool for quantification of nonalcoholic fatty liver disease. In this work, a protocol of plane wave quantitative ultrasound (QUS) and shear wave elastography imaging (SWEI), quasi-simultaneously acquired, dedicated to quantification of liver steatosis on *in vivo* fatty duck liver is presented. Shear wave velocity was estimated to classify stiffness in duck liver tissue. QUS consisted of local attenuation coefficient slope estimated with Spectral Log Difference method, and coherent-to-diffuse signal ratio computed from homodyned-K parametric maps. After 9 days of feeding, US attenuation reached a maximum and coherent-to-diffuse signal ratio reached a minimum. Coupled together, QUS and SWEI promise a strong potential in steatosis monitoring of fatty liver tissue, in ducks or humans.**

Keywords— Quantitative ultrasound (QUS), shear wave elastography imaging (SWEI), steatosis, fatty liver, duck

I. Introduction

Non-alcoholic fatty liver disease (NAFLD) is one of the most prevalent liver disease in Western countries, affecting 20-30% of the general adult population and an estimated 200 million individuals with an advanced form known as non-alcoholic steatohepatitis (NASH) [1]. Current clinical practices include biopsies, computed tomography, or magnetic resonance imaging for NAFLD diagnosis.

Ultrasound techniques may allow cost effective imaging and are promising for early steatosis grading and prognosis [2]. However, ultrasound techniques do not estimate fat fraction directly but instead provide physical biomarkers such as tissue viscoelasticity, ultrasound attenuation, speed of sound, spectral backscattering properties, or scatterers' acoustical properties and spatial organization through echo-envelope statistics as an indirect measure of fat content. Multi-parametric methods have recently offered the promise of increasing the diagnostic performance accuracy for steatosis, NASH and fibrosis classification by coupling elastography with spectral based features for tissue characterization [3].

In this study, fat growth in 16 mulard ducks' liver, which were being raised for commercial *foie-gras* production, was investigated during their mechanical-feeding. The mulard ducks (*Anas platyrhynchos domesticus* × *Cairina moschata*) have the ability to develop extreme but reversible steatosis under controlled mechanical-feeding of *foie gras* production, which has been well reported in the literature [4,5]. The liver fat fraction can rise from negligible to as high as 60% in only two weeks of mechanical feeding.

The main purpose of this study was to design an *in vivo* duck liver multi-parametric ultrasound imaging protocol that can be utilized during mechanical feeding. The portability of the ultrasound scanners made it possible to perform the ultrasound imaging sessions directly at a farm for liver steatosis monitoring.

II. Methods

A. Animal Procedure

Sixteen mulard ducks housed in a farmhouse were included in this study. The study was approved by the Institutional Animal Care Committee of the University of Montreal Hospital Research Center. The feeding process was planned in two parts: pre-feeding for 16 days (from d-15 to d0), followed by 16 days of mechanical-feeding (from d1 to d16). During the mechanical feeding process, the ducks were fed twice a day with an increasing amount of re-humidified full corn grains over the complete duration (approx. 350 g per feeding at the beginning and 650 g at the end, composed of 40% water and 60% dried corn grains). Imaging sessions were conducted at four time points along the feeding process (d-10, d2, d9 and d16). During the experiments, the animals were awake and a veterinarian handled them to perform ultrasound scans in the

farmhouse. A small patch of feathers were plucked off the outer skin over the liver's position and cleaned up with water and alcohol before applying acoustic coupling gel for ultrasound imaging. At the end of the feeding duration, animals were sent to a slaughterhouse where further industrial process would be followed in view of commercialization.

B. Ultrasound Acquisitions

Ultrasound data acquisitions were performed in the farmhouse with the help of a veterinarian using a portable research ultrasound system (Verasonics V1 programmable scanner, Verasonics, Kirkland, WA, USA) and an ATL L7-4 linear probe with central frequency of 5 MHz (Philips, Bothell, WA, USA). The acoustic push centre under the duck skin and the fat layers were manually selected at a depth of at most 1 cm within the liver. Each acquisition recorded 100 plane wave frames at 3.086 kHz frame rate for QUS imaging. It was immediately followed by focusing 3 acoustic pushes similar to SSI, lasting 198.4 µs each and separated by 2.5 mm in depth for SWEI, where 100 frames were acquired at a rate of 3.623 kHz for shear wave tracking. Each animal underwent two to four acquisitions in one session. Figure 1(a) represents a schematic diagram of the experiments. A separate reference acquisitions for QUS were carried out on an industrial reference 117GU-101 CIRS phantom (Norfolk, VA, USA – α_{ref} = 0.72 dB.cm^{-1}.MHz^{-1}, BSC$_{ref}$(3 MHz) = 1.24 10^{-3} str^{-1}.cm^{-1}).

C. Shear Wave Speed Estimation

The Young's modulus of the tissue can be computed from the phase velocity, c_φ , as $E = 3\rho {c_\varphi}^2$, where ρ is the mass density of the medium. Shear wave phase velocity was estimated to characterize the stiffness using linear fitting of the phase function at 400 Hz shear wave frequency along lateral position *x,* as detailed in [6]. A square region-of-interest (ROI) measuring 1 cm ×1 cm was selected within the imaged liver tissue assuming a homogeneous purely elastic medium [7], and phase velocity was estimated within this ROI. The quality of the linear fit of the phase velocity function was assessed via the coefficient of determination (R^2) for goodness-of-fit estimation. The estimated shear wave velocity was accepted for $R^2 > 0.9$ [8]. For each duck and imaging session, the estimated Shear Wave Speed (SWS) values meeting this criterion were averaged out to a single value of shear wave speed.

D. Local Attenuation Coefficient Slope Estimation

Local attenuation coefficient slope (ACS) was estimated with spectral log difference (SLD) method as described in [9]. Radiofrequency (RF) beamformed data were averaged over the acquired 100 frames. The parameter estimation region (PER) size was selected to be 20 scan lines in lateral direction, and 40 pulse lengths in axial direction. The proximal and distal windows within PER were 20 pulse lengths long the axial direction. The overlap was 75% in lateral direction and 87.5% in axial direction. The ACS maps were averaged over the segmented liver region for each acquisition. Finally, ACS values were averaged to provide a single value of ACS per duck per imaging session.

E. Coherent-to-diffuse ratio Estimation

The statistical distribution of the echo envelope of the RF signals [10] was modelled with the homodyned K-distribution as explained in [11, 12]. A sliding window of 140×17 pixels^2, approximately 5 mm × 5 mm in axial and lateral directions, was swept across the segmented region within liver by steps of 7×1 pixels^2, and computations were performed within the sliding window as explained in [13, 14]. Readers may refer to [14-17] for more details on homodyned-K features estimation. In this work, the analysis was presented for the parameter- k, the coherent-to-diffuse signal ratio, which is related to the presence of structure within spatial organization of scatterers, or the presence of specular reflection. The mean and interquartile range (IQR) were computed and their median values over all frames are reported.

III. Results

Results are presented in Figure 1, where it can be observed that all estimated features individually exhibited significant trends ($p < 10^{-3}$, Kruskal-Wallis rank-sum test) during the mechanical-feeding. Changes can be observed after only 2 days of mechanical-feeding (d-10 to d2) indicating the beginning of pathological changes in tissue structure. Figure 1(b) shows increment in shear wave speed over the feeding period. As can be observed from the figure, after the completion of mechanical feeding process the average shear wave speed in the duck livers had doubled from 0.94 ± 0.09 m/s to 1.89 ± 0.19 m/s.

Figure 1(c) and (d) present changes in local ACS and coherent-to-diffuse signal ratio during the mechanical feeding process. After 9 days of mechanical feeding, attenuation reached a maximum, and coherent-to-diffuse signal ratio reached a minimum. In fact, the increase in local ACS was from 0.64 ± 0.08 dB/cm/MHz at d2 to 0.91 ± 0.11 dB/cm/MHz at d9, but it then decreased to 0.69 ± 0.07 dB/cm/MHz at d16. A similar behavior was observed with coherent-to-diffuse signal ratio. The behavior of these features suggest a change in the nature of scatterers and could be due to microscopic changes occurring at cellular scale during the steatosis process with fat fraction as high as 60%.

Furthermore, the number of SWEI acquisitions per session that could be utilized ($R^2 \geq 0.9$ criterion for linear fit) for the shear wave speed computation decreased along the mechanical feeding process showing a degradation of the SWS estimation. This might be caused by the

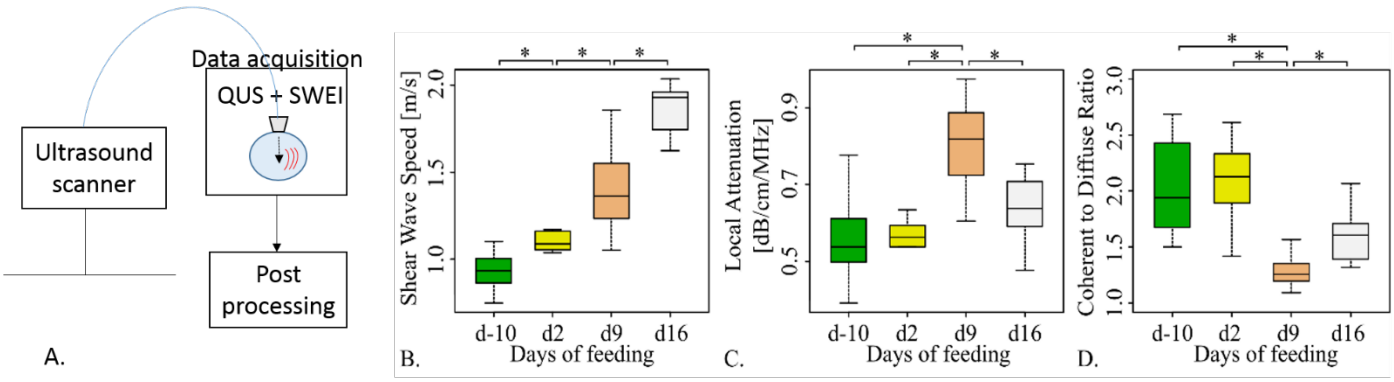

Figure 1. QUS+SWEI imaging of duck fatty liver. A. Schematic representation of the experiment. Sixteen duck livers are imaged in-vivo during mechanical-feeding process. B. C. and D. (resp.) Shear wave speed, local attenuation coefficient slope and coherent-to-diffuse signal ratio in duck livers during feeding process. 'd-10' stands for 10 days before the start of the mechanical feeding. (*$p<10^{-3}$)

measurement noise arising due to pushing beam defocusing by fat intake which resulted in energy loss. Thus, even though shear wave speed estimation provided a monotonic trend and an interesting classification performance within its own limitations, it cannot be reliably used exclusively in thick fat tissues due to the greater amount of unreliable data along the process. Thus, coupling of SWEI with QUS together may promote a strong potential in steatosis grading, and paves way for human liver studies.

IV. Discussion

The effects of controlled liver fat intake on state-of-the-art ultrasound biomarkers in healthy to heavily steatosed duck livers were investigated in 16 mulard ducks *in vivo*. It was hypothesized that the duck liver was homogeneous and estimated features were averaged over the segmented region. SWEI results disclosed that shear wave speed almost doubled since the first acquisition was performed at the beginning of pre-feeding to the last acquisition performed after 16 days of mechanical feeding. This suggests that stiffness of duck *foie-gras* is distinguishably higher than healthy duck liver [18].

Local attenuation coefficient slope trend was observed to be increasing up to day 9 and then decreased as the fat amount grew in excessive quantity. An explanation could be found in the paper by Davies et al [19] where a similar lack of attenuation was reported in three excessively fatty human liver clinical cases. The causes were hypothesised to be lying in the changes in the cellular structure of the liver that occur due to high fat accumulation.

Plane wave ultrasound imaging was preferred in this study after considering the unavoidable movement of ducks during image acquisitions. It was hypothesised that the experiments could benefit from the rapidity of acquisitions provided by plane wave imaging, in spite of its lower SNR. Furthermore, it was recently shown that QUS with plane wave imaging was viable [20], and that angular compounding can increase the frame rate, while signal quality can be retained along with stabilized spatial variability [21].

Low variance estimators have also been developed in the recent literature [22,23], and future study could involve development of features that account for spatial heterogeneity of duck fatty liver or human non diffusing liver diseases.

The method presented in this work can be translated to human clinical trials on NASH. However, some of the trends observed in this study may vary, such as stiffness in steatosis [6,24], due to the obvious distinction in the fat intake induced in 2 weeks in duck liver versus a disease that can take a much longer time in humans to appear. Finally, the limitation of the proposed study may lie in the cost associated with it. Availability of a dedicated veterinarian, especially in a small farm, for non-invasive detection of *foie-gras* in a duck before slaughtering for industrial purposes may not be realistic. A simpler equipment such as Fibroscan® can be utilized to estimate CAP and stiffness in liver which may be more suitable for industrial needs.

V. Conclusion

This study presented a multi-parametric ultrasound imaging workflow for steatosis monitoring in ducks that were being raised for commercial *foie-gras* production. Shear wave elastography imaging and quantitative ultrasound imaging acquisition were performed in 16 mulard ducks in a farmhouse to develop biomarkers for better classification and grading. The observed trends in shear wave speed, local ultrasound attenuation coefficient slope, and coherent-to-diffuse signal ratio along the mechanical feeding process were reported. It is envisaged that the protocol developed in this study can be utilized in human clinical studies that may pave the way for better fatty liver prognosis.

Acknowledgments

This work was supported by an Audace grant number 2019-AUDC-263591 from the Fond de Recherche du Québec. Authors thank Fernande Ouellet and Francis Laroque, *foie gras* producers from the farm "Rusé comme un canard", and Nathalie Vermette, veterinarian, who performed the ultrasound examinations. An Tang is supported by a Clinical Research Scholarship from the Fonds de recherche du Québec en Santé (FRQ-S) and Fondation de l'association des radiologistes du Québec (FARQ) (FRQS-ARQ #34939).

References

[1] K. Sharma et al., "Attenuation of shear waves in normal and steatotic livers," Ultrasound Med. Biol., vol. 45, pp. 895-901, 2019.

[2] Y. N. Zhang et al., "Liver fat imaging—a clinical overview of ultrasound, CT, and MR imaging," Br. J. Radiol., vol. 91, pp. 20170959, 2018.

[3] E. Franceschini et al., "Quantitative ultrasound in ex vivo fibrotic rabbit livers," Ultrasound Med. Biol., vol. 45, pp. 1777-1786, 2019.

[4] E. Baéza, C. Marie-Etancelin, S. Davail, and C. Diot, "La stéatose hépatique chez les palmipèdes," INRA Prod. Anim., vol. 26, pp.403–414, 2013.

[5] L. Locsmándi, G. Hegedüs, G. Andrássy-Baka, F. Bogenfürst, and R. Romvári, "Following the goose liver development by means of cross-sectional digital imaging, liver histology and blood biochemical parameters," Acta Biol. Hung., vol. 58, pp. 35-48, 2007.

[6] T. Deffieux et al., "Investigating liver stiffness and viscosity for fibrosis, steatosis and activity staging using shear wave elastography," J. Hepatol., vol. 62, pp. 317-324, 2015.

[7] S. Chen, M. Fatemi, and J. F. Greenleaf, "Quantifying elasticity and viscosity from measurement of shear wave speed dispersion," J. Acoust. Soc. Am., vol. 115, pp. 2781-2785, 2004.

[8] F. T. H. Yu, E. Franceschini, B. Chayer, J. K. Armstrong, H. J. Meiselman, and G. Cloutier, "Ultrasonic parametric imaging of erythrocyte aggregation using the structure factor size estimator," Biorheology, vol. 46, pp. 343-363, 2009.

[9] T. A. Bigelow and Y. Labyed, "Attenuation Compensation and Estimation", in *Quantitative Ultrasound in Soft Tissues*, J. Mamou and M. L. Oelze, Ed., Dordrecht Heidelberg New York London: Springer, 2014, pp. 71-94.

[10] F. Kallel, M. Bertrand, and J. Meunier, "Speckle motion artifact under tissue rotation," IEEE Trans. Ultrason. Ferroelectr. Freq. Control, vol. 41, pp. 105-122, 1994.

[11] V. Dutt and J. F. Greenleaf, "Ultrasound echo envelope analysis using a homodyned k distribution signal model," Ultrason. Imaging, vol. 16, pp. 265-287, 1994.

[12] F. Destrempes and G. Cloutier, "A critical review and uniformized representation of statistical distributions modeling the ultrasound echo envelope," Ultrasound Med. Biol., vol. 36, pp. 1037-1051, 2010.

[13] F. Destrempes and Cloutier G, "Review of envelope statistics models for quantitative ultrasound imaging and tissue characterization", in *Quantitative Ultrasound in Soft Tissues*, J. Mamou and M. L. Oelze, Ed., Dordrecht Heidelberg New York London: Springer, 2014, pp. 219-274.

[14] F. Destrempes, J. Porée and G. Cloutier, "Estimation method of the homodyned K-distribution based on the mean intensity and two log-moments", SIAM J. Imaging Sci., vol. 6, pp. 1499-1530, 2013.

[15] F. Destrempes, E. Franceschini, F. T. H. Yu, G. Cloutier, "Unifying concepts of statistical and spectral quantitative ultrasound techniques," IEEE Trans. Med. Imaging, vol. 35, pp. 488-500, 2016.

[16] M. H. Roy-Cardinal, F. Destrempes, G. Soulez, and G. Cloutier, "Assessment of carotid artery plaque components with machine learning classification using homodyned-K parametric maps and elastograms," IEEE Trans. Ultrason. Ferroelectr. Freq. Control, vol. 66, pp. 493-504, 2018.

[17] A. Tang, F. Destrempes, S. Kazemirad, J. Garcia-Duitama, B. N. Nguyen, and G. Cloutier, "Quantitative ultrasound and machine learning for assessment of steatohepatitis in a rat model," Eur. Radiol., vol. 29, pp. 2175-2184, 2018.

[18] M. Bhatt et al., "Reconstruction of viscosity maps in ultrasound shear wave elastography," IEEE Trans. Ultrason. Ferroelectr. Freq. Control., vol. 66, pp. 1065-1078, 2019.

[19] R. J. Davies, S. H. Saverymuttu, M. Fallowfield, and A. E. A. Joseph, "Paradoxical lack of ultrasound attenuation with gross fatty change in the liver," Clin. Radiol. vol. 43, pp. 393–396, 1991.

[20] J. Garcia-Duitama et al., "Experimental application of ultrafast imaging to spectral tissue characterization," Ultrasound Med. Biol., vol. 41, pp. 2506-2519, 2015.

[21] S. Salles et al., "Experimental evaluation of spectral-based quantitative ultrasound imaging using plane wave compounding," IEEE Trans. Ultrason. Ferroelectr. Freq. Control, vol. 61, pp. 1824-1834, 2014.

[22] A. L. Coila and R. J. Lavarello, "Regularized spectral log difference technique for ultrasonic attenuation imaging," IEEE Trans. Ultrason. Ferroelectr. Freq. Control, vol. 65, pp. 378-389, 2018.

[23] Z. Vajihi, I. M. Rosado-Mendez, T. J. Hall, and H. Rivaz, "Low variance estimation of backscatter quantitative ultrasound parameters using dynamic programming," IEEE Trans. Ultrason. Ferroelectr. Freq. Control, vol. 65, pp. 2042-2053, 2018.

[24] K. Nightingale et al., "Derivation and analysis of viscoelastic properties in human liver: Impact of frequency on fibrosis and steatosis staging," IEEE Trans. Ultrason. Ferroelectr. Freq. Control, vol. 62, pp. 165-175, 2015.